The 2016 World Congress on
Advances in Civil, Environmental, and Materials Research (ACEM16)
Jeju Island, Korea, August 28-September 1, 2016

Case Study of Wind-Induced Performance of Long-Span Bridges under Typhoon Conditions Considering Higher Turbulence Intensity and Unsteady Admittance Function

*Lin Zhao[1)] and Yaojun Ge[2)]

[1), 2)] *Key Laboratory for Disaster Reduction in Civil Engineering, Tongji University, Shanghai 200092, China*
[1)] *zhaolin@tongji.edu.cn*

ABSTRACT

Through applying passive turbulence generators in TJ-3 wind tunnel, 1:100 reduced-scale wind field of type B terrain was re-illustrated under typhoon and normal conditions, and wind-induced aero-elastic performance tests of Xihoumen suspension bridge were carried out as well. Furthermore, aerodynamic admittance function about cross section in mid-span main girder under the condition of higher turbulence intensity of typhoon field was identified via using high-frequency force-measured balance. Furthermore, based on improved aerodynamic admittance expressions, Wind-induced stochastic vibration of Xihoumen bridge under typhoon and normal climates were calculated and compared, considering structural geometrical non-linearity, stochastic wind attach angle effects, etc. Thus, the aerodynamic response characteristics under typhoon and normal conditions can be illustrated and checked, which are of satisfactory response results for different incoming wind velocities with resemblance to those wind tunnel testing data under the two types of climate modes.

1. INTRODUCTION

At present, wind-induced vibration theory and wind-resistant structural design usually base themselves on normal climate, in other words, non-typhoon condition, such as monsoon and cold snap. Wind field parameters, including gust factor, profiles concerning mean wind and turbulent intensity, turbulent integral scale, wind spectrum equation etc., are mainly related to monsoon condition in non-typhoon regions. However, it's well known that many high-rise buildings and long-span bridges located in typhoon-prone coastline areas are very sensitive to typhoon dynamic action through some investigation about the on-site measurements and wind tunnel tests (Xu and Zhan 2001, Li et al. 2002, Campbell et al. 2005, Li et al. 2004, 2008), and wind environment parameters and wind-induced vibration characteristics during typhoons

[1), 2)] Professor

also differ from normal climates. The indication is that turbulent intensity and gust factor nearby the ground could be larger than predefined values from Chinese wind loading Codes, the slope ratios of mean wind profile under typhoon less than corresponding values in normal condition (Mikitiuk and Isyumov 1994, Amano et al. 1999, John and Chou 2001). As expected, design wind loading and wind-excited responses of flexible structures are also quite different between the two types of climate modes (Pande et al. 2002, Zhu 2002, Eamon et al. 2007, Ge and Zhao, 2014). Despite the western Pacific Ocean region, including southeastern coast of China and most of Korea and Japan, are seriously affected by strong typhoons with the highest recorded wind velocities, investigations about typhoon dynamic action on high rise buildings and long-span bridges are so deficient that it has posed a thorny problem to the structural engineers.

2. AERODYNAMIC LOADING

The aerodynamic forces acting on 2-D line-like cross-section of bridge girder or arch can be formulated as

$$M\ddot{X} + C\dot{X} + KX = F_G + F_{st} + F_b + F_{se} \tag{1}$$

in which M, C, and K are mass, damping and stiffness matrix. X is displacement vector, including lateral, vertical and torsional movements. F_G, F_{st}, F_b and F_{se} are gravity, static wind force, stochastic buffeting force and self-excited aerodynamic force, respectively.

The motion-dependent aero-elastic forces distributed on unit span of bridge girder are expressed as a linear function of nodal displacement and nodal velocity (Jain et al. 1996). The effect of self-excited force, describing complicated interference between moving cross-section and atmospherical flow, can be equivalently treated as combination about aerodynamic stiffness and aerodynamic damping (Namini 1991), like this,

$$F_{se} = K_{se}X + C_{se}\dot{X} \tag{2}$$

$$M\ddot{X} + (C - C_{se})\dot{X} + (K - K_{se})X = F_G + F_{st} + F_b \tag{3}$$

in which aerodynamic stiffness and damping matrix can be expressed as

$$\left[K_{se}^{i}\right]_l = \rho U^2 L_e K_{cr}^2 \begin{bmatrix} 0 & 0 & 0 & 0 & 0 & 0 \\ 0 & H_4 & H_6 & BH_3 & 0 & 0 \\ 0 & P_6 & P_4 & BP_3 & 0 & 0 \\ 0 & BA_4 & BA_6 & B^2A_3 & 0 & 0 \\ 0 & 0 & 0 & 0 & 0 & 0 \\ 0 & 0 & 0 & 0 & 0 & 0 \end{bmatrix} \tag{4}$$

$$\left[C_{se}^{i}\right]_{I}=\rho UBL_{e}K_{cr}\begin{bmatrix}0&0&0&0&0&0\\0&H_{1}&H_{5}&BH_{2}&0&0\\0&P_{5}&P_{1}&BP_{2}&0&0\\0&BA_{1}&BA_{5}&B^{2}A_{2}&0&0\\0&0&0&0&0&0\\0&0&0&0&0&0\end{bmatrix} \tag{5}$$

where ρ is air density, U is oncoming mean wind velocity, K_{cr} is reduced frequency matrix, B and L_e are width and length items of moving cross-section, P_i*, H_i* and A_i* are flutter derivatives for lateral, vertical and torsional movements. For the sake of brevity, some detailed derived steps are ignored. The commercial software ANSYS has provided a kind of special element types, MATRIX27, which could be defined by customers so that we can utilize this convenience to realize the above mentioned aerodynamic stiffness and damping effects through the additory couple MATRIX27 elements at the end of realistic elements to describe the self-excited aerodynamic force effect (Fig.1).

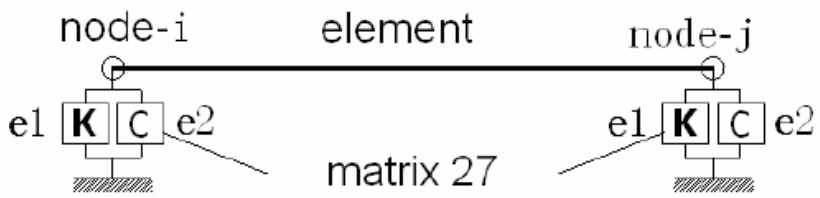

Fig.1 Additory aerodynamic MATRIX27 element on structural element

At present, the wind-induced stochastic buffeting analysis is still based on quasi-steady theory considering admittance function modification. Traditional Liepmann's approximation to Sears function derived from thin plate and streamline aerofoil, or so-called maximal value 1.0 approximated as the possible upper limitation are usually applied in practical engineering application. In this investigation, the wind induced response have prominent role in the wind excited performance of long-span suspension bridge, especially for flexible main girder, so more attentions about admittance function identification and application is only focused on along wind aerodynamic loads. The buffeting force expressions in time-domain and frequency-domain about cross section (i.e. lift force) can be written as

$$L_b(t)=1/2\,\rho U^2\left(B\,2C_L\chi_u\frac{u(t)}{U}+(C_L'+C_D)\chi_w\frac{w(t)}{U}\right) \tag{6}$$

$$S_L(\omega)=\rho^2U^2B^2\left(C_L^2(\alpha)\left|\chi_{Lu}\right|^2S_u(\omega)+1/4\left(C_L'(\alpha)-C_L(\alpha)\right)^2\left|\chi_{Lw}\right|^2S_w(\omega)\right) \tag{7}$$

in which L is Lift buffeting force, C means static aerodynamic coefficient, C' defines the derivative to wind attack angle, χ represents aerodynamic admittance function, u and w are horizontal and vertical fluctuating wind components.

Sears function was originally derived from thin aerofoil in isotropy flow field, but most of bridge cross sections have the characteristics of blunt body, more or less, so we have to face the doubt concerning whether or not the Sears function deriving from streamline structures is still suitable for blunt parts in long-span bridge structures (Zhao, et al. 2016). Considering the absence of time-domain admittance formula, an alternative method can be used: firstly, modify the wind spectrum expressions $S_u(\omega)$ and $S_w(\omega)$ by multiplying admittance function in frequency-domain, that are $\left|\chi_{Lu}\right|^2 S_u(\omega)$ and $\left|\chi_{Lw}\right|^2 S_w(\omega)$; then, change modified wind spectrum into time history using harmonic wave combination technique. Stochastic wind history along main girder in Xihoumen Bridge was numerical simulated. Based on the requirement from Wind Loading Codes from various countries, the correlation between longitude and vertical wind component is assumed to be non-correlated, and coherence function about different spatial points for longitude or vertical direction are set to follow the relationship like. In order to simulate spatial points stochastic wind histories simultaneously, improved Deodatis algorithm are used, which is the commonly-used algorithm and can guarantee the simultaneous simulation about stochastic process.

For the convenience of usability, equivalent expression (lift item shown as examples) about multi-components admittance function have been proposed as:

$$\left|\varphi_{LL}(K)\right|^2 = \frac{4C_L^2(\alpha)\left|\chi_{Lu}\right|^2 S_u(K) + \left(C_L' - C_L\right)^2 \left|\chi_{Lw}\right|^2 S_w(K)}{\left(4C_L^2(\alpha) S_u(K) + C_L'^2 S_w(K)\right)} \tag{8}$$

in which, $\left|\varphi_{LL}(K)\right|^2$ is equivalent admittance in lift force direction, $\left|\chi_{Lu}\right|^2$ and $\left|\chi_{Lw}\right|^2$ define the crisscross admittance components regarding u and w direction. So, the lift spectrum can be changed into the simplified expression

$$S_L(\omega) = \rho^2 U^2 B^2 \left|\varphi_{LL}(K)\right|^2 \left(4C_L^2(\alpha) S_u(\omega) + \left(4C_L'(\alpha) + C_D(\alpha)\right)^2 S_w(\omega)\right) \tag{9}$$

The $\left|\varphi_{LL}(K)\right|^2$ can be identified using high-frequency force-measured balance and be fitted using double logarithm coordinate third-order multinomial as

$$\log_{10}(F(\omega)) = \sum_{i=0}^{3}\left(a_i \log_{10}{}^i(\omega B/U)\right) \tag{10}$$

where a_i are fitting parameters, ω defines circular frequency. The goal spectrum $\left|\varphi_{LL}(K)\right|^2 S_u(\omega)$ and $\left|\varphi_{LL}(K)\right|^2 S_w(\omega)$, which are modified with equivalent admittance function, can be changed into fluctuating wind history by using harmonic wave combination method, and the stochastic wind time-domain signal $\chi_{Lu}u(t)$ and $\chi_{Lw}w(t)$ can be finally obtained. In fact, the phasic angle information about oncoming wind dynamic action are more or less ignored in the above conversion process, however, the statistical results of wind induced response are still of rationality.

4. CASE STUDY OF ENGINEERING APPLICATION

In this study, Xihoumen suspension bridge, located in southeastern coast of China, belonging to typical typhoon-prone regions, is selected as numerical examples, shown as Figs.2-3. Series of wind tunnel tests have been conducted in Tongji wind tunnel, and the full-scale aeroelastic model with 1:100 reduced-scale ratio was also designed and manufactured in TJ-3 wind tunnel, shown as Fig. 4. The basic design and aerodynamic parameters concerning Xihoumen Bridge are presented in Table 1. The static wind coefficient and aerodynamic derivatives for various wind velocities and wind attack angles are identified basing on 2-D cross section wind tunnel tests like other most commonly-used wind-resistance procedures.

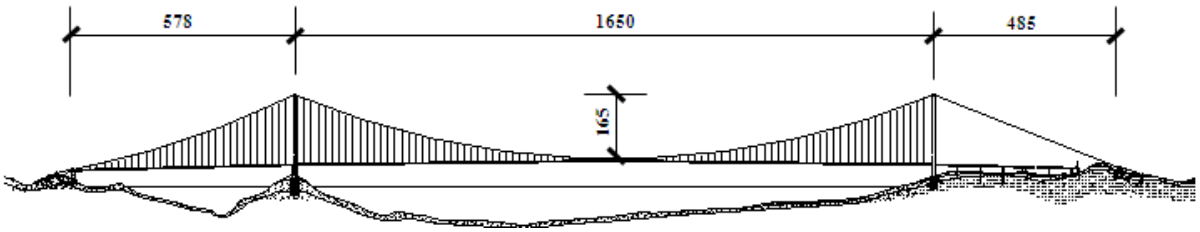

Fig. 2 Layout of Xihoumen Bridge

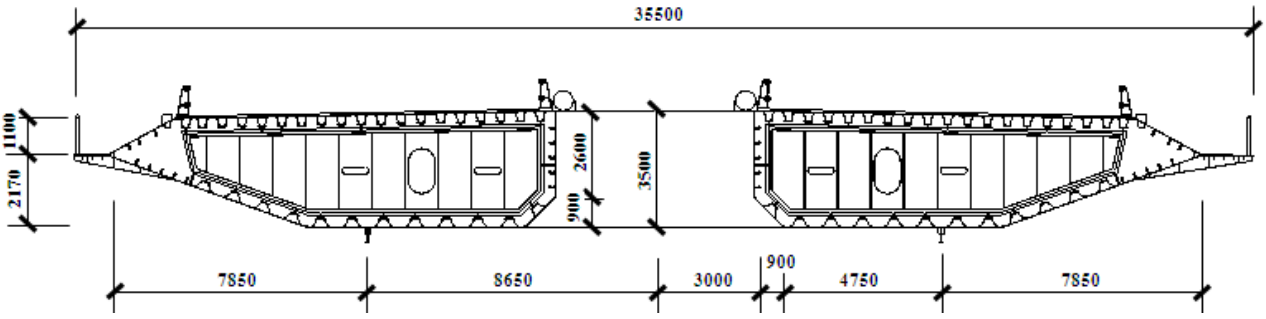

Fig. 3 Cross-section of Xihoumen Bridge girder

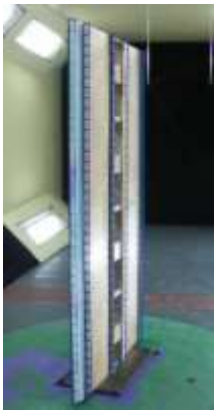

a) Static wind coefficient-measured tests

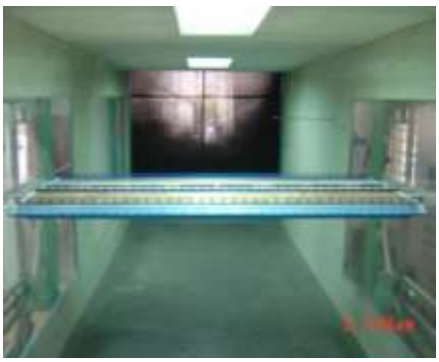

b) Vibration-measured tests

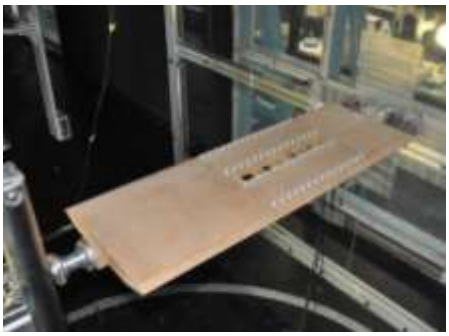

c) Admittance identified tests

d) Full bridge aeroelastic tests

Fig. 4 Series of wind tunnel tests

Table 1 Basic parameters about Xihoumen Bridge

Structral type		1650m suspension bridge			
Elevation of main girder (m)		54.0			
Sizes of main girder		Girder in middle span			
		Width (m)		Height (m)	
		35.5		3.5	
Type of vibration		Vertical bending	Lateral bending	Torsion	
Dynamic characters	Frequency (Hz)	0.100	0.049	0.232	
	Damping ratio	9.3‰		6.0‰	
Static wind parameter		Lift	Drag	Torque	
0° attack angle	Mean	-0.050	0.104	0.011	
	Slope	2.264	-0.028	0.218	
Self-excited aerodynamics		Lift		Torque	
Flutter derivatives of attack angle 0°		H1	H4	A2	A3
Main derivatives		-1.805	0.588	-0.071	0.146

To investigate the effects of climate mode on wind-induced vibration quantitatively, the case study about Xihoumen Bridge are therefore carried out. Firstly, the passive turbulent generators, such as triangle and rectangle spine and various roughness blocks are used in TJ-3 wind tunnel to re-illustrate the 1:100 reduced-scale wind fields about Type B terrain under normal and typhoon conditions, and mean wind velocity and turbulent intensity profile are in good agreement with Codes definition during normal climate and Monte-Carlo predicted values about typhoon modes.

Table 2 Wind-induced displacement RMS of Xihoumen Bridge under 0° attack angle

Type of climate	Methods	Admittance function	Middle span		Quarter point	
			Vertical bending (m)	Torsion (°)	Vertical bending (m)	Vertical bending (m)
Normal	Wind tunnel tests		0.320	0.139	0.280	0.118
	FEM calculation	1.0	0.729	0.421	0.694	0.380
		Sears	0.513	0.218	0.463	0.198
		Identified admittance	0.368	0.145	0.312	0.132
Typhoon		1.0	0.549	0.269	0.585	0.244
		Sears	0.369	0.112	0.273	0.101
		Identified admittance	0.385	0.162	0.330	0.133

The wind spectrum in TJ-3 under normal and typhoon conditions were also measured and compared with standard spectrum suggested by Chinese wind loading Codes. Usually, the turbulence intensity under typhoon condition is larger than those under normal climate for various heights from the ground. For the normal condition, there is obviously coincidence between measured spectrum and standard spectrum (Simiu and Panofsky spectrum, see Eqs. (9)-(10)). However, for the typhoon condition, though integral value about non-dimensional power spectrum intensity function along the reduced frequency coordinate has the same value that is 1.0 like those under normal condition, another changing tendencies show the wind field characteristics during typhoon climate. It is easily found that spectrum intensity is lower than corresponding value in the lower frequency of normal wind field, and in the higher frequency scope, spectrum intensity values of typhoon field are larger than those of normal field.

Then, the wind-excited performance about Xihoumen aeroelastic model was measured under typhoon and normal climate modes. In order to improve the precision of numerical simulation, the equivalent admittance functions of main girder are also identified using dynamic force measured testing system and recognized algorithm. It's obvious that the realistic results of calculation based on identified admittance function about main girder are different from Sears function to some extent (see Table 2), showing the importance role of admittance for improving the precision of calculation.

5. CONCLUSIONS

Xihoumen long-span bridge was selected to conduct serial case study analysis. For cross section of Xihoumen main girder, admittance function about 2-D section was identified, then full bridge aero-elastic model tests are carried out in TJ-3 wind tunnel under two climate modes. Moreover, wind-excited response was computed considering some structural and aerodynamic nonlinearity under normal and typhoon climates. Since the traditional admittance treatment, such as analytical Sears function or 1.0, may over- or under-estimate wind-induced response, and admittance function depends

on flow turbulence intensity for two types of climate mode, it's necessary to utilize measured admittance function based on wind tunnel tests to improve prediction precision about wind-excited performance.

REFERENCES

Amano, T., Fukushima, H., Ohkuma, T., Kawaguchi, A. and Goto, S. (1999), "The observation of typhoon winds in Okinawa by Doppler sodar", *Journal of Wind Engineering and Industrial Aerodynamics*, **83**, 11-20.

Campbell, S., Kwok, K.C.S. and Hitchcock, P.A. (2005), "Dynamic characteristics and wind-induced response of two high-rise residential buildings during typhoons", *Journal of Wind Engineering and Industrial Aerodynamics*, **93**, 461–482.

Ge, Y.J., and Zhao, L. (2014), "Wind-excited stochastic vibration of long-span bridge considering wind field parameters during typhoon landfall", *Wind and Structures*, **19**(4), 421-441.

Jain, A., Jones, N.P. and Scanlan, R.H. (1996), "Coupled flutter and buffeting analysis of long-span bridges", *Journal of Structural Engineering*, 1**22**, 716-725.

John, Z.Y. and Chou, C.R. (2001), "A study of the characteristic structures of strong wind", *Atmospheric Research*, **57**, 151–170.

Li, Q.S., Xiao, Y.Q., Wong, C.K. and Jeary, A.P. (2004), "Field measurements of typhoon effects on a super tall building", *Engineering Structures*, **26**, 233-244.

Li, Q.S., Xiao, Y.Q., Wu, J.R., Fu, J.Y. and Li, Z.N. (2008), "Typhoon effects on super-tall buildings", *Journal of Sound and Vibration*, **313**, 581-602.

Li, Z.X., Chan, T.H.T. and Ko, J.M. (2002), "Evaluation of typhoon induced fatigue damage for Tsing Ma", *Engineering Structures,* **24**, 1035–1047.

Mikitiuk, M. and Isyumov, N., etc. (1994), "The Wind Climate for Shanghai, PRC.", The University of Western Ontario, *Engineering Science Research Report*, BLWT-SS35-1994.

Namini, A.H. (1991), "Analytical modeling of flutter derivatives as finite elements", *Computers & Structures*, **41**, 1055-1064.

Pande, M., Ho, T.C.E., Mikitiuk, M., Kopp, G.A. and Surry, D. (2002), "Implications of Typhoon York on the design wind speeds in Hong Kong", *Journal of Wind Engineering and Industrial Aerodynamics*, **90**, 1569-1583.

Xu, Y.L. and Zhan, S. (2001), "Field measurements of Di Wang Tower during Typhoon York", *Journal of Wind Engineering and Industrial Aerodynamics*, **89**, 73-93.

Zhao, L. and Ge, Y.J. (2015), "Cross-spectral recognition method of bridge deck aerodynamic admittance function", *Earthquake Engineering and Engineering Vibration,* **14**(4), 595-609.

Zhu, L.D. (2002), "Buffeting Response of Long Span Cable-supported Bridges under Skew Winds", Ph.D. Dissertation ,The Hong Kong Polytechnic University, Hong Kong.

Zhu, L. D., Zhao L., Ge, Y.J. and Cao, S.Y. (2012), "Validation of numerical typhoon model using both near-ground and aerial elevation wind measurements". *Disaster Advances*. **5**(1), 14-23.